

DYNAMIC STALL MODELING AND CORRELATION WITH
EXPERIMENTAL DATA ON AIRFOILS AND ROTORS

R. G. Carlson, Supervisor
R. H. Blackwell, Dynamics Engineer
Rotor Dynamics Section
Sikorsky Aircraft Division of United Aircraft Corporation
Stratford, Connecticut

G. L. Commerford, Research Engineer
Aeroelastics Group, Fluid Dynamics Laboratory
United Aircraft Research Laboratories
East Hartford, Connecticut

P. H. Mirick, Aerospace Engineer
U. S. Army Air Mobility Research and Development Laboratory
Fort Eustis, Virginia

Abstract

Two methods for modeling dynamic stall have been developed at United Aircraft. The α , A, B Method generates lift and pitching moments as functions of angle of attack and its first two time derivatives. The coefficients are derived from experimental data for oscillating airfoils. The Time Delay Method generates the coefficients from steady state airfoil characteristics and an associated time delay in stall beyond the steady state stall angle. Correlation with three types of test data shows that the α , A, B Method is somewhat better for use in predicting helicopter rotor response in forward flight. Correlation with lift and moment hysteresis loops generated for oscillating airfoils was good for both models. Correlation with test data in which flexibly mounted two-dimensional airfoils were oscillated to simulate the LP pitch variation of a helicopter rotor blade showed that both methods overpredicted the response, and neither gave a clear advantage. The α , A, B Method gave better correlation of torsional response of full scale rotors and remains the method in general use. The Time Delay Method has the potential to be applied more easily and probably can be improved by consideration of spanwise propagation of stall effects.

Stall-related phenomena limit the operational capabilities of the helicopter. Power, blade stress, and control system loads can all increase substantially due to blade stall. To predict such phenomena unsteady aerodynamics in stall must be modeled in blade aeroelastic analyses. A number of unsteady aerodynamic models have been developed. These include methods described in References 1 and 2. Reference 3 is a recent general survey article of rotor dynamic stall. The α , A, B Method and the Time Delay Method are two methods developed by United Aircraft. The α , A, B Method was developed to use airfoil test data obtained for a sinusoidally oscillating

Presented at the AHS/NASA-Ames Specialists' Meeting on Rotorcraft Dynamics, February 13-15, 1974.

Based on work performed under U. S. Army Air Mobility Research and Development Laboratory Contract No. DAAJ02-72-C-0105.

two-dimensional model airfoil. The Time Delay Method was developed to provide an empirical method that would agree with the lift and pitching moment hysteresis characteristics measured in oscillating airfoil tests for a number of airfoils and test conditions.

Evaluation of unsteady aerodynamic modeling techniques generally proceeds from correlation with data obtained in two-dimensional oscillating airfoil tests to correlation of full scale rotor blade torsional response. Two-dimensional rigid airfoil results are compared on the basis of aerodynamic pitch damping and lift and pitching moment hysteresis loops, and full scale correlation is judged on the basis of agreement in blade torsional moments or control rod loads. Evaluation of an unsteady model on the basis of full scale torsional response is made difficult by uncertainties in three-dimensional rotor inflow and blade bending and plunging motion. Correlation of the lift and pitching moment time histories of rigidly driven airfoils, on the other hand, is not the best method of comparison because it does not treat blade dynamic response to stall. As an intermediate approach, model test data were obtained for a flexibly mounted model airfoil which was dynamically scaled to simulate the dynamics of the first torsional mode of a rotor blade. This paper summarizes unsteady aerodynamic modeling techniques and includes comparisons based on two-dimensional aerodynamic pitch damping, lift and pitching moment hysteresis loops, two-dimensional flexured airfoil response, and full scale rotor blade torsional moments.

Description of the Unsteady Models

α , A, B Method

In the α , A, B method the aerodynamic moment is assumed to be a function of angle of attack and its first two time derivatives. Reference 4 demonstrated that unsteady normal force and moment data generated during sinusoidal airfoil tests and tabulated as functions of α , $A = \frac{b\dot{\alpha}}{U_0}$ and $B = \frac{b^2\ddot{\alpha}}{U_0^2}$

(where b is the airfoil semi-chord and U_0 is the free stream velocity) could be used to predict the aerodynamic response of an airfoil executing

a nonsinusoidal motion. In a limited number of flexured airfoil tests described in Reference 4, good correlation was achieved between measured and predicted airfoil dynamic response. The α , A, B lift and pitching moment data tabulations of Reference 4 were used in the calculation of torsional response for the dynamically scaled model airfoil. As applied in this investigation, two changes were made in the calculation. First, to consider the pitch axis of the model airfoil as a variable, provision was made to include pitching moment due to chordwise offset of the aerodynamic center from the pitch axis:

$$c_{m_{\bar{X}_{PA}}}(\alpha, A, B) = c_{m_c/4}(\alpha, A, B) + (\bar{X}_{PA} - .25)c_l(\alpha, A, B)$$

The second change involved scaling the unsteady data tables to account for differences in wind tunnel characteristics. The steady state lift and moment data for the present test program differed from the corresponding steady data obtained in Reference 4 because the tests were conducted in an open jet wind tunnel and because the airfoil effective aspect ratio was much higher. The method of scaling used for these analyses required a shift in the entire data tabulation by constant values of angle of attack, unsteady lift coefficient, and unsteady moment coefficient according to the following relations:

$$c_l(\alpha, A, B)_{\text{open jet}} = c_l(\alpha + \delta\alpha_l, A, B)_{\text{TAB}} + \delta c_l$$

and

$$c_m(\alpha, A, B)_{\text{open jet}} = c_m(\alpha + \delta\alpha_m, A, B)_{\text{TAB}} + \delta c_m$$

The constants $\delta\alpha_l$, $\delta\alpha_m$, δc_l and δc_m were established for each airfoil and were equal to the amount of shift necessary to make the open jet steady state stall points in lift and moment match the steady state stall points of the airfoil of Reference 4.

Time Delay Unsteady Model

Wind tunnel airfoil dynamic response was also calculated with the Sikorsky Time Delay unsteady aerodynamic method. This formulation was developed empirically by generalizing the results of a set of oscillating airfoil test programs. It is intended to predict the unsteady aerodynamic characteristics of arbitrary airfoils. Its aim is to provide the blade designer with unsteady lift and pitching moment characteristics of various airfoils without conducting extensive oscillating airfoil tests. This model, based on a hypothesis of the physical separation process, does not depend on an assumed harmonic variation of angle of attack. The basic assumption is that there exists a maximum quasi-static angle of attack at which the pressure distribution and the boundary layer are in equilibrium. During increases in angle of attack beyond this static stall angle, there are finite time delays before a redistribution of pressure causes first a moment

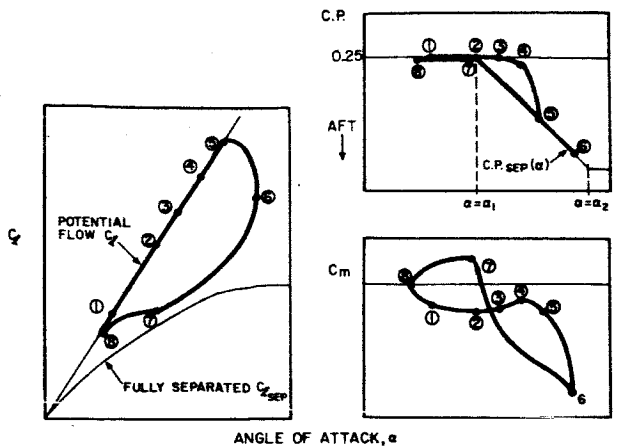
break and then a loss of lift corresponding to flow separation. The relative phasing of the moment and lift breaks with angle of attack produces either positive or negative damping of the motion.

To test the Time Delay hypothesis, harmonic data from Reference 5 were examined. It was noted that the onset of stall can occur before, with, or after maximum amplitude of the oscillation. In accordance with the Time Delay hypothesis, the spread between the static moment stall angle and the dynamic lift break was evaluated in terms of elapsed time nondimensionalized by free stream velocity and chord length, $\tau^* = \Delta t_{\text{SEP}}(U_o/c)$.

Typical results show that separation generally occurs when τ^* exceeds about 6.

Dynamic pitching moment stall has been handled similarly. Test data showed, in general, that the dynamic moment break occurred before the lift break. This has been noted in Reference 6 and attributed to the shedding of a vortex at the airfoil leading edge at the beginning of the separation process. Rearward movement of the vortex over the surface of the airfoil tends to maintain lift, but drastically alters the pitching moment.

To apply the Time Delay Model to a given airfoil, only static aerodynamic data are required. First, the airfoil static lift and pitching moment data are used to define the approximate variation in center of pressure between the static moment stall angle α_s and an angle of attack α_2 above which the center of pressure is assumed fixed. Secondly, an approximation is made to the c_l versus α curve for fully separated flow. The sequence of events occurring during one stall-unstall cycle is detailed in Figure 1. Briefly stated, lift and pitching moment are determined from potential flow theory until the nondimensional time τ_2 (which begins counting when the angle of attack exceeds the static moment stall angle) reaches τ_1 . At this point the pressure distribution begins to change, leading to rearward movement of the center of pressure and loss of potential flow pitching moment. Later, when $\tau_2 = \tau^*$, the lift breaks from the static line and decreases gradually with time to the fully separated value, $c_{l_{\text{SEP}}}(\alpha)$. For $\tau_2 > \tau^*$ the center of pressure coincides with C.P._{SEP}(α). At the point where $\dot{\alpha} = 0$, the rates at which c_l approaches $c_{l_{\text{SEP}}}(\alpha)$ and C.P. approaches C.P._{SEP}(α) (if it does not already equal C.P._{SEP}(α)) are increased. When α falls back below the quasi-static stall angle α_1 , the center of pressure returns to the quarter chord, potential flow pitching moment effects are reintroduced and a second time parameter τ_3 is recorded to govern the rate at which c_l returns to $c_{l_{\text{POT}}}$.



- ① $\alpha < \alpha_1$
 - $c_l = c_{lPOT}$
 - C.P. = 0.25
 - $c_m = c_{mPOT} = -\frac{\pi}{4} \frac{d\delta}{dt}$
- ② $\alpha = \alpha_1$
 - τ_2 counting begins $\tau_2 = \sum_{n=0}^{\infty} \Delta t_n \frac{U_{on}}{c}$ at $\alpha = \alpha_1$
- ③ $\tau_2 =$ moment stall time constant $\tau_B = 2.0$
 - C.P. begins to move rearward with time toward C.P._{SEP}(α)
 - c_{mPOT} is eliminated
- ④ $\tau_B < \tau_2 < \tau^*$
 - c_l remains equal to c_{lPOT}
 - C.P. continues to shift aft with time, τ_2
 - $C.P. = 0.25 + \frac{(\tau_2 - \tau_B)}{(\tau^* - \tau_B)} [C.P._{SEP}(\alpha) - 0.25]$
 - $c_m = c_l(C.P. - 0.25)$
- ⑤ $\tau_2 =$ lift stall time constant $\tau^* = 6.0$
 - c_l begins to decay toward $c_{lSEP}(\alpha)$
 - $c_l = c_{lPOT} - [c_{lPOT} - c_{lSEP}(\alpha)] [1 - e^{-(\tau_2 - \tau^*)/4}]$
 - C.P. moves to C.P._{SEP}(α) independent of subsequent variation in α
- ⑥ $\dot{\alpha} = 0$
 - the exponential rate at which c_l approaches $c_{lSEP}(\alpha)$ is increased by a factor of 3
 - if $\tau_B < \tau_2 < \tau^*$ the rate at which C.P. approaches C.P._{SEP}(α) is increased by doubling the time increment
 - $\tau_{2n+1} = \tau_{2n} + 2\Delta t_n \left(\frac{U_{on}}{c}\right)$
- ⑦ $\alpha < \alpha_1$
 - τ_3 counting begins $\tau_3 = \sum_{n=0}^{\infty} \Delta t_n \left(\frac{U_{on}}{c}\right)$ at $\alpha = \alpha_1, \dot{\alpha} < 0$
 - c_l moves back toward c_{lPOT}
 - C.P. returns to 0.25
 - potential flow moment is reintroduced $c_m = c_{mPOT} e^{-\tau_3/4}$
- ⑧ $\dot{\alpha} = 0$
 - $\tau_2 = \tau_3 = 0$
 - $c_l = c_{lPOT}$
 - C.P. = 0.25
 - $c_m = c_{mPOT}$

Figure 1. Time Delay Unsteady Aerodynamic Model.

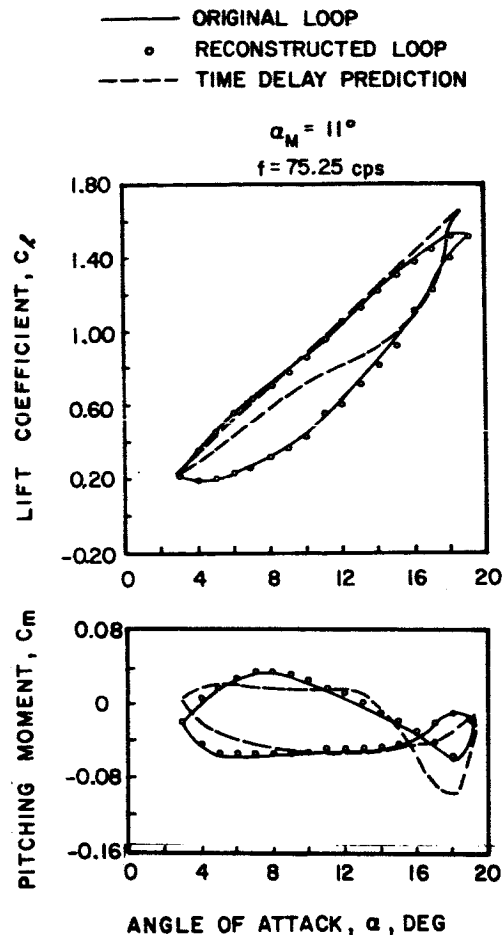


Figure 2. Correlation with NACA 0012 Lift and Pitching Moment Hysteresis Loops.

Although additional correlation studies must be made to identify the effects of airfoil type on the time delay constants and although refinements to the present model may be implemented, this rather simple model represents well the essential features of the dynamic stall process. Correlation typical of that claimed for other empirical methods (References 2 and 7) has been found with data from References 4, 5, and 8. Only the α, A, B Method has produced better correlation (Reference 4), but it suffers from the requirement for extensive testing and data processing. Figure 2 compares the NACA 0012 unsteady lift and pitching moment hysteresis loops measured in Reference 4 with Time Delay results. This correlation was achieved by setting the lift break time constant τ^* equal to 4.0 instead of 6.0. Three-dimensional effects encountered in this test apparently reduced the time interval between static stall and dynamic lift stall. Also shown are the hysteresis loops

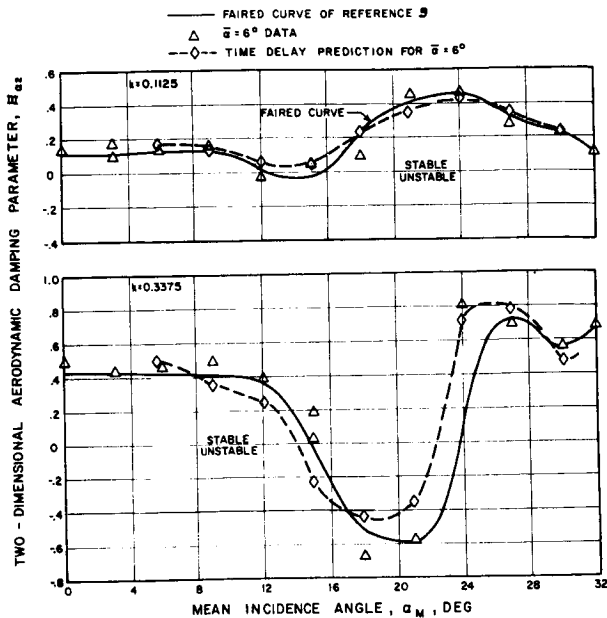


Figure 3. Correlation of Two-Dimensional Aerodynamic Pitch Damping.

predicted using the α , A, B Method. The α , A, B Method correlation is with the data from which the α , A, B coefficients were derived.

In addition to predicting the exact form of lift and moment hysteresis loops, an unsteady model should represent faithfully aerodynamic pitch damping. Accordingly, the Time Delay Model was used to calculate two-dimensional aerodynamic damping for the reduced frequency/mean angles of attack test points of Reference 9. Sample results plotted versus airfoil mean incidence angle of attack are shown in Figure 3. Generally excellent correlation of measured and predicted damping is noted.

Other correlation of the Time Delay Method with two-dimensional oscillating airfoil test data has been good. During development of the theory, correlation was carried out with forced oscillating airfoil data for a range of airfoils, frequencies of forced oscillation, Mach numbers, and angles of attack. Typical examples of the correlation obtained are shown in Figure 4 where measured and calculated hysteresis loops are shown for the V13006-7 airfoil. These test data taken from Reference 1 show the correlation with the Boeing Theory of Reference 1 as well. Correlation included hysteresis loops for different airfoils and covered a Mach number range from 0.2 to 0.6. In all cases, the general character and magnitude of the hysteresis loops were well matched. In particular, the method provides the sharp drop in pitching moment that is often found when stall occurs. The oscillation frequency in

Figure 4 is constant for the two cases, but Mach number and mean angle of attack are changed. The lift break occurs before the angle of attack reaches its maximum value. In terms of the non-dimensional time parameter τ^* , the τ^* value of 6 at which lift stall occurs is reached before the maximum angle of attack is reached. The Time Delay and Boeing Methods show comparable correlation for lift. For the Mach number 0.4 case (Figure 4b) the return to potential flow occurs earlier for decreasing angle of attack than the return given by the Time Delay Method. Pitching moment correlation is better for the Time Delay Method. The triple loop characteristic is well duplicated. Similar correlation obtained with the Time Delay Method for a wide range of conditions demonstrated its promise as a practical method for analyzing unsteady aerodynamics.

Dynamic Stall Tests

In order to obtain data useful in evaluating the two unsteady aerodynamic methods dynamic stall wind tunnel tests were run using a two-dimensional airfoil model. The model was oscillated at a frequency simulating the cyclic pitch variation on a helicopter rotor blade. Torsional frequencies representative of helicopter blade frequencies were obtained by varying a torsional stiffness element between the drive system and the airfoil section. The airfoil models were made to be as stiff as possible along their span and light in weight to approximate scaled helicopter blade mass and inertia properties. Hence the non-dimensional coefficients in the equation of motion of the model airfoil were close to those of the helicopter blade torsional equation of motion based on the aerodynamics of the three-quarter radius on the retracting blade. Two different airfoils were fabricated, an NACA 0012 and an SC 1095.

The model airfoils and drive system were designed to permit investigation of the effects on torsional response of torsional natural frequency, chordwise pitch axis location and torsional inertia over a range of 1P frequencies for an NACA 0012 airfoil and a cambered SC 1095 airfoil. The oscillating mechanism provided an 8-degree amplitude of motion of the model with an adjustable mean angle of attack. The model has a span of 1.75 feet and a chord of 0.5 feet. The wind tunnel velocity was 275 fps for all tests. Time histories of the model angular motion were recorded at nominal driving frequencies of 8.0, 10.0, and 12.5 cps. Tests were run for the full range of angle of attack for all the combinations of pitch axis, torsional inertia, torsional natural frequency, and airfoil type. A typical set of time histories for a basic reference condition (NACA 0012 airfoil, 25 percent pivot axis, nominal blade inertia, and 5P natural frequency ratio) is shown for four mean angles of attack in Figure 5. These time histories represent the time average of ten cycles.

The elastic torsional deflection of the airfoil (difference between total angular motion and input angular motion) was obtained for each test condition by subtracting the input angular

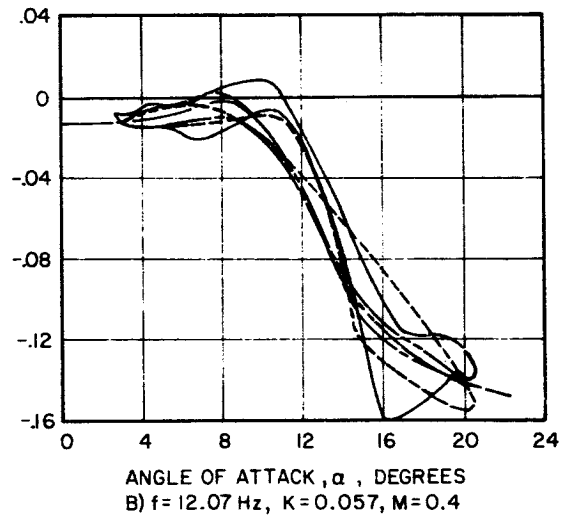
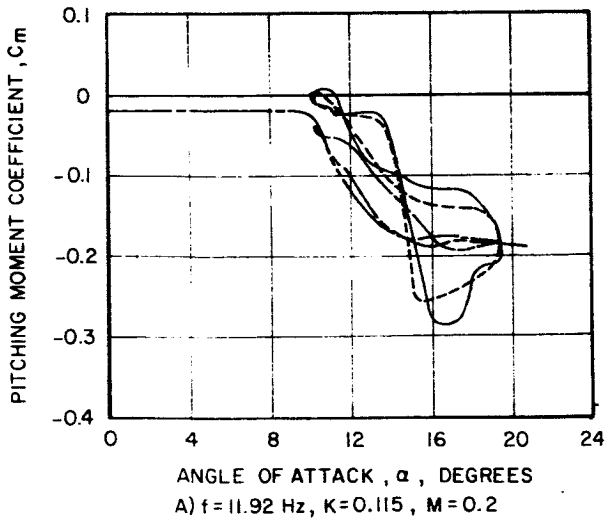
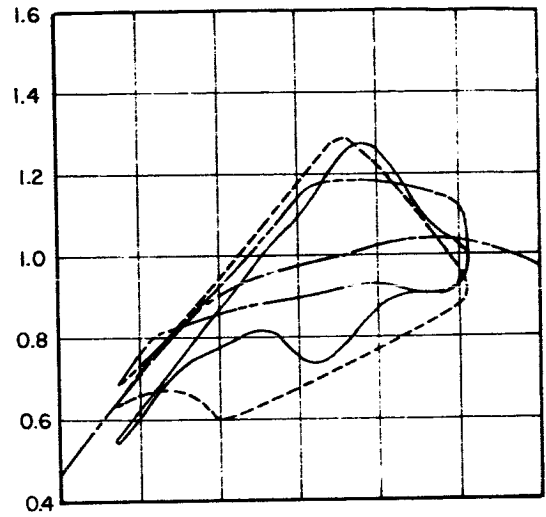
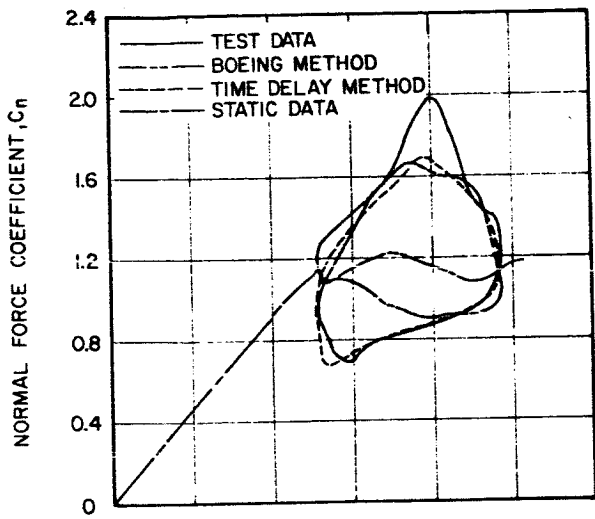


Figure 4. Correlation of Dynamic Loops for the V13006-7 Airfoil in Forced Pitch Oscillation.

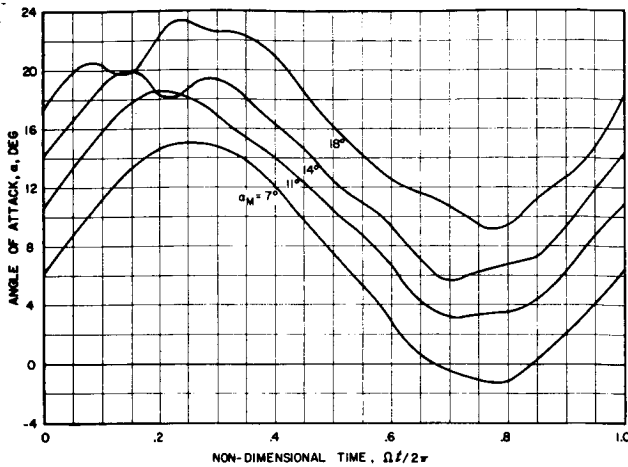


Figure 5. Averaged Time Histories of Angle of Attack for the Model Airfoil.

position time history from the averaged airfoil angular position time history:

$$\theta(\tau) = \alpha(\tau) - (\alpha_m + \bar{\alpha} \sin 2\pi\tau)$$

where $\theta(\tau)$ is the difference between the measured non-dimensional angular time history response $\alpha(\tau)$ and the input driving motion. The non-dimensional time τ is given by t/T , where the period, T , was established from the ten-cycle time-averaging process for that run. Some statistical variation in measured response was noted when stall flutter occurred, but in general the ten cycle time averaged response was representative of the

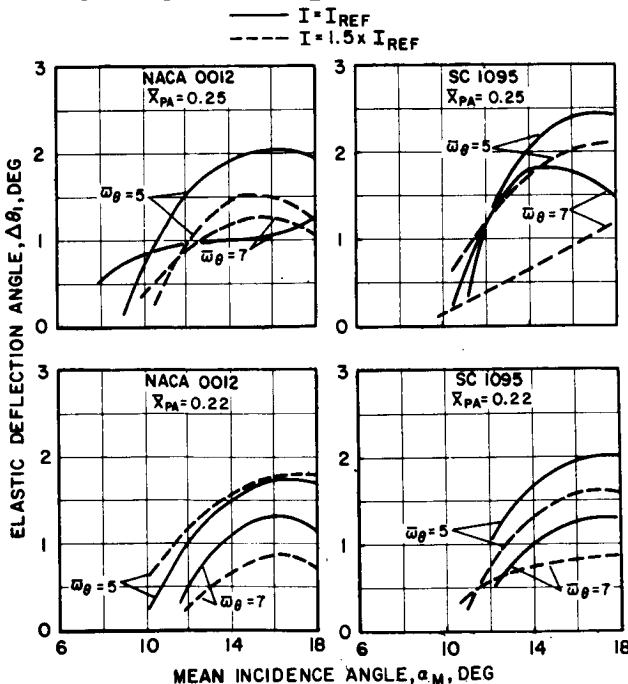


Figure 6. Model Airfoil Elastic Deflection.

measured data. Two measures of stall response amplitude were extracted from each of the $\theta(\tau)$ time histories. These were $\Delta\theta_1$ which is one-half of the initial response to stall and $\theta_{1/2PTP}$ which is one-half of the overall peak-to-peak elastic deflection.

It was found that the initial stall response parameter $\Delta\theta_1$ gave the most consistent indication of susceptibility to stall flutter. The possible reduction in flutter amplitude introduced by the time averaging procedure when there was cycle-to-cycle variation in phase made it somewhat difficult to assess the amplitude of flutter response. Fortunately, the initial stall deflection showed virtually no cycle-to-cycle variation. Figure 6 compares measured initial deflection angles for an excitation frequency Ω of 10 cps for the two airfoils at all combinations of airfoil natural frequency ratio ($\bar{\omega}_\theta = \omega_\theta/\Omega$), torsional inertia, and pitch axis. Certain general trends of deflection angle can be identified in the test results.

1. Elastic deflection increases with mean incidence angle.
2. For the same torsional inertia, response is generally greater for the lower frequency airfoil section.
3. The amplitude of response is inversely related to torsional inertia.
4. Forward movement of the pitch axis leads to a decrease in deflection.
5. SC 1095 airfoil dynamic stall response begins to build up at a higher mean incidence angle than the 0012, but the two airfoils have comparable responses once stall is penetrated.

Correlation Study of Two-Dimensional Results

The two-dimensional flexured airfoil test data were compared with predictions based on various unsteady aerodynamic methods. The single torsional degree of freedom differential equation of motion for the flexibly mounted airfoil section oscillating in the wind tunnel test section is given by

$$I\ddot{\alpha} + c\dot{\alpha} + K(\alpha - \alpha_m) = M(t) + K\bar{\alpha} \sin \Omega t$$

where c = equivalent mechanical damping per unit span

I = airfoil torsional inertia per unit span

K = torsional spring constant

M_t = applied aerodynamic moment

t = time

α = airfoil angle of attack

$\bar{\alpha}$ = amplitude of angular oscillation

ω_m = mean angle of the oscillation

Ω = angular frequency of the applied torque

This equation was solved numerically using the unsteady aerodynamic models to calculate the applied aerodynamic moment $M(t)$. For the α , A , B Method unsteady data tables obtained from earlier oscillating airfoil tests, Reference 4, were scaled for both airfoils. The measured steady state lift

and pitching moment data served as inputs in the Time Delay calculations. Additionally, the airfoil mean incidence angle used in the Time Delay solution was two degrees less than that set in the wind tunnel. The open jet flow deflection experienced at high unsteady lift coefficients was sufficient to decrease actual peak angles of attack to a value somewhat lower than the geometrically impressed pitch angle. The two-degree correction to α_M gave consistently better correlation of the initial stall time.

Correlation between measured wind tunnel model response and response calculated with the unsteady models was examined for thirty-six test conditions. The set of cases studied was sufficient to evaluate the independent effects on airfoil stall response of mean incidence angle,

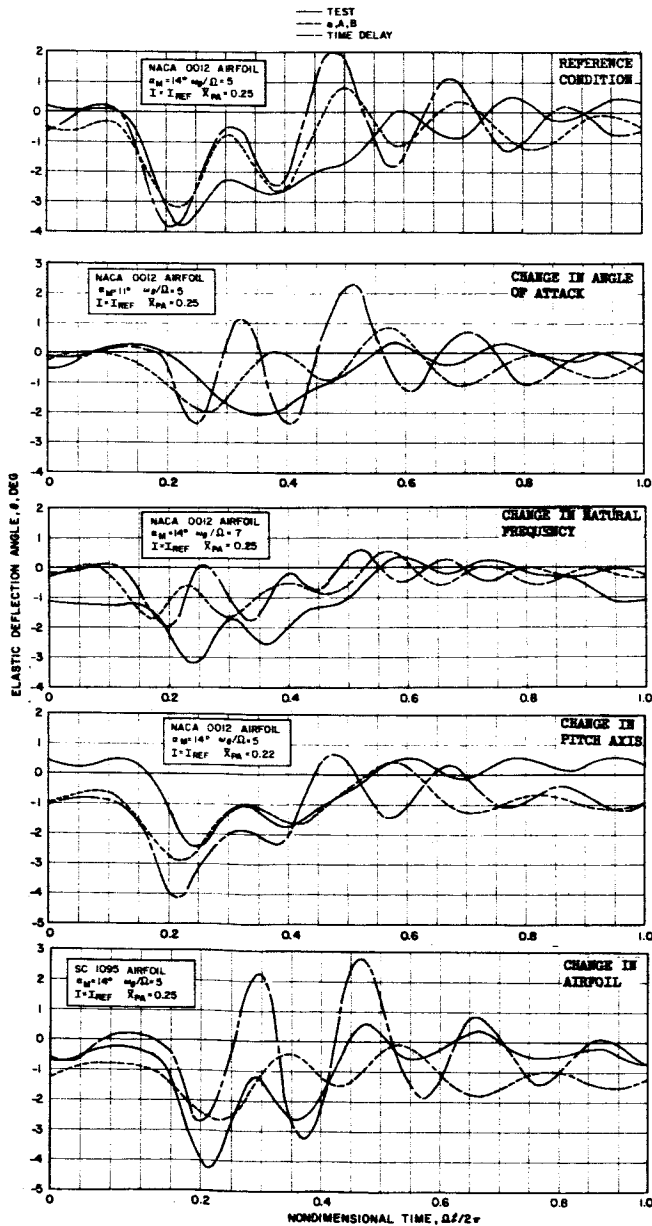


Figure 7. Effect of Parameters on Airfoil Response.

torsional natural frequency, chordwise pitch axis, torsional inertia, and airfoil type. Relative to a baseline case taken to be the NACA 0012 airfoil at $\alpha_M = 14^\circ$, $\omega_0/\Omega = 5$, $X_{PA} = 0.25$, and $I = I_{REF}$, Figure 7 shows measured and predicted effects of mean angle, torsional natural frequency, pitch axis, and airfoil type on time histories of elastic deflection. Comparison of the measured and predicted effects of airfoil mean angle of attack indicates that deeper penetration into stall results in sharper initial stall deflection and larger residual stall flutter response. The two analyses predict these effects qualitatively, but each - especially the Time Delay model - overpredicts the amplitude of response. The main effects of an increase in torsional natural frequency are a shift in response frequency and a decrease in the amplitude of elastic deflection. Figure 7 shows good correlation of response amplitude, although both analyses predict an initial stall response earlier than that measured. Moving the airfoil pitch axis forward causes delay in initial stall time and reduction in amplitude of response. The analytical results do predict the reduction in response amplitude, but the Time Delay model still results in overpredicted response. Finally, a comparison between the NACA 0012 and the SC 1095 airfoils shows a delay in the initial stall time for the SC 1095 airfoil, which had a static stall angle measured in this wind tunnel to be about three degrees higher than that of the NACA 0012. However, the SC 1095 stall flutter amplitude was comparable to that experienced by the NACA 0012 at this condition.

The time history correlation was good in that the initial response and the frequency of the subsequent oscillations were predicted. The trends observed in test were well matched by the analysis, although the Time Delay model generally overpredicted stall flutter response. The basic effects of structural changes on blade response time histories were well predicted by either analysis.

Although torsional elastic deflection is important in determining rotor stability and performance, the torsional moments resulting from stall flutter are the designer's primary concern. To measure the trends of torsional moment with parameter changes, the twisting moment experienced by the flexible connector in the model airfoil drive system was calculated for each test condition. The torsion moment M_θ was calculated using the equivalent spring stiffness of the connector:

$$M_\theta = K_{eq} \theta = (I_{airfoil} \omega_\theta^2) \theta$$

The torsional moments corresponding to the initial stall deflection angle $\Delta\theta_1$ were used to show the effects of blade parameters on structural moments. Figure 8 presents typical results for three combinations of airfoil type and mean angle of attack. It was generally found that decreasing torsional natural frequency reduced stall flutter moments. Although the stiffer system experienced lower response amplitudes, the corresponding structural moments were increased:

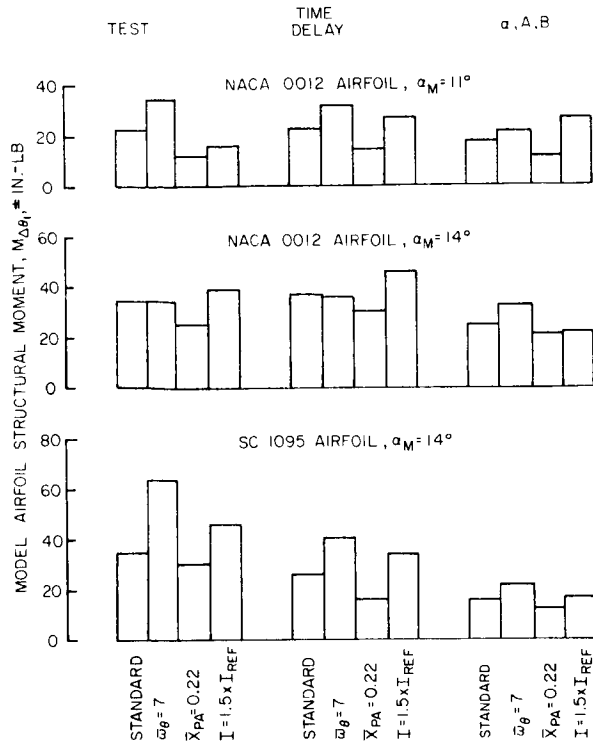


Figure 8. Effect of Airfoil Parameters on Model Airfoil Vibratory Torsional Moments.

$$\frac{M_{\theta 7p}}{M_{\theta 5p}} = \left(\frac{\omega_{\theta 7p}}{\omega_{\theta 5p}} \right)^2 \left(\frac{\bar{X}_{PA 7p}}{\bar{X}_{PA 5p}} \right) = \left(\frac{7}{5} \right)^2 \left(\frac{\bar{X}_{PA 7p}}{\bar{X}_{PA 5p}} \right)$$

Forward placement of the airfoil pitch axis generally decreased vibratory torsional moments. The two analyses predicted this trend with comparable accuracy. That forward movement of the airfoil pitch axis relative to the aerodynamic center reduces stall flutter moments can be understood based on lift and pitching moment hysteresis loops. For an airfoil with pitch axis forward of the center of pressure, positive lift forces cause negative moments about the pitch axis. For positive lift, the lift hysteresis loop is usually traversed in the clockwise direction, which contributes a negative pitching moment loop in the counterclockwise (stabilizing) direction. A decrease in torsional moment amplitude with decreasing torsional inertia was generally found throughout the testing. This trend, evident in two of the conditions shown in Figure 8, is predicted somewhat more correctly by the Time Delay Analysis. Finally the two airfoils are compared in Figure 9. For two different combinations of inertia and pitch axis, high stall flutter moments are delayed in mean angle with the SC 1095 airfoil.

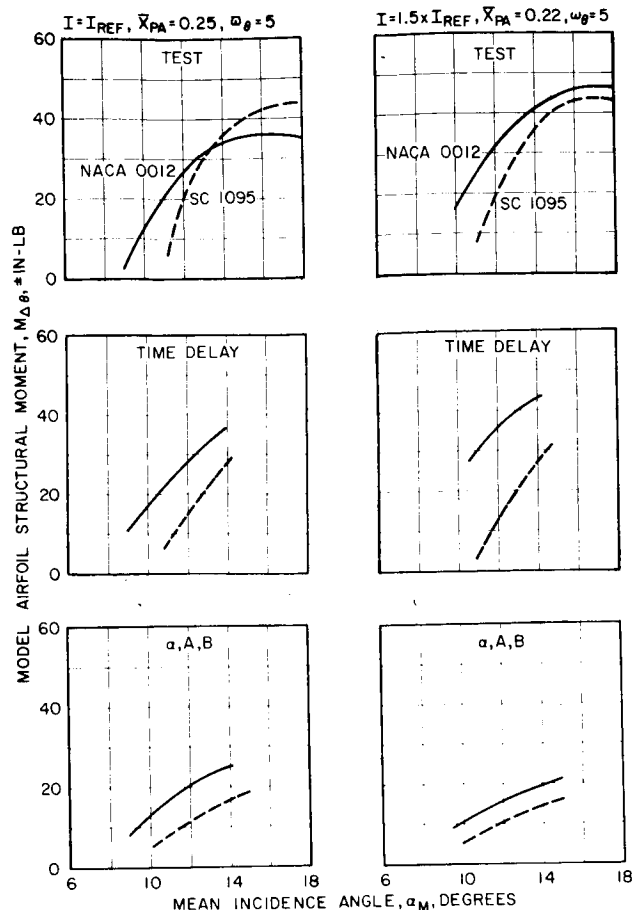


Figure 9. Effect of Airfoil Type on Structural Moments

Flight Test Correlation

Flight test data were correlated with the Normal Modes Blade Aeroelastic Analysis for both the CH-53A and CH-54B aircraft. Both models of unsteady aerodynamics were used. Information on the blade analysis used can be found in Reference 10.

Correlation of CH-53 control system loads, blade stresses and required power was studied at a nominal aircraft gross weight of 42,000 lb ($C_m/\sigma = 0.083$), a tip speed of 710 ft/sec, and a 3000 ft density altitude for airspeeds ranging from 100 knots to 170 knots. Inclusion of variable inflow was found to be essential in calculating the proper levels of blade bending moments. It also provided some improvement in the correlation of blade torsional moments.

The α , A, B and Time Delay aerodynamic models are compared at 137 knots in Figure 10. Figures 10a and 10b shows that the computed blade stresses are comparable for the two methods. However, the push rod loads calculated with the Time Delay Model are much less than values calculated with the α , A, B Method and measured values. The Time

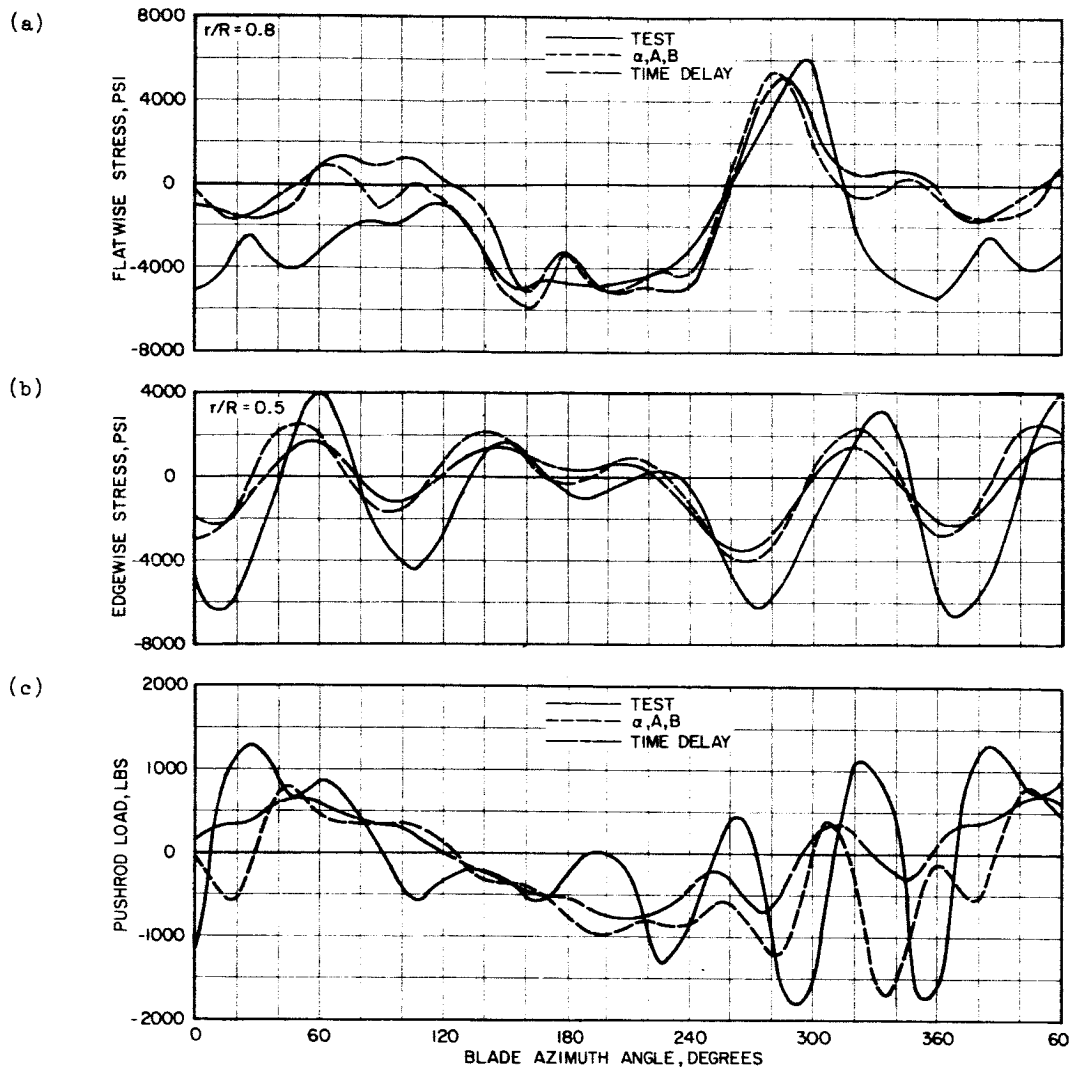


Figure 10. Correlation of CH-53A Blade Stresses and Pushrod Loads.

Delay results generally do not give sufficiently large oscillations in stall.

That better correlation of stall flutter moments was possible with the α, A, B Method is evident in Figure 11a which shows the buildup of vibratory pushrod load amplitude with airspeed. The α, A, B model predicts a buildup rate almost identical with the mean of the test data. A discrepancy of no more than 10 knots in the knee of the control load curve is evident at this thrust coefficient. Figure 11b shows the correlation of pushrod load amplitude achieved with the α, A, B Method at three thrust coefficients.

Calculated CH-54B control loads were also generally less than measured values. Figure 12 indicates that a definite stall boundary is pre-

dicted by the analysis. Relative to the CH-53A calculations, a decreased control load stall speed and an increased rate of buildup with airspeed are clearly predicted. Again, higher loads are computed based on the α, A, B Model. The comparison of measured and predicted push rod load time histories indicates that the α, A, B results reflect a buildup in the higher frequency loads much more accurately than do the Time Delay calculations.

It is not entirely clear why, relative to the α, A, B method, the Time Delay model underpredicts helicopter control loads while overpredicting the stall flutter oscillations of the two-dimensional wind tunnel model. Examination of several blade section pitching moment/angle of attack hysteresis loops indicates not so much

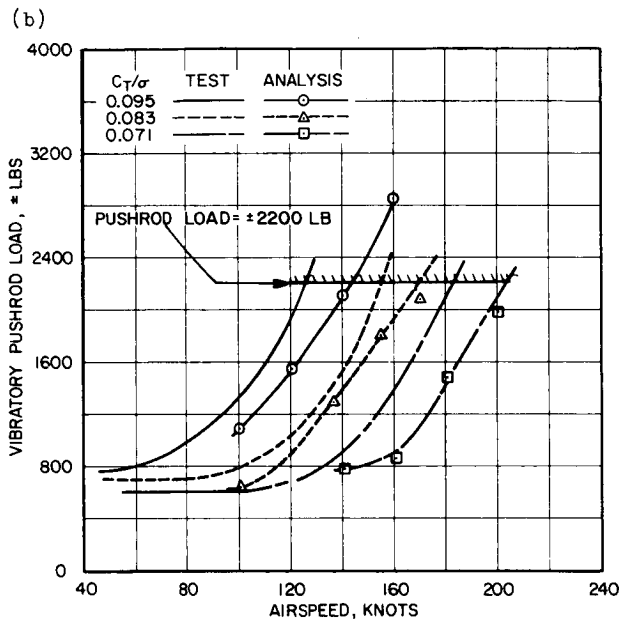
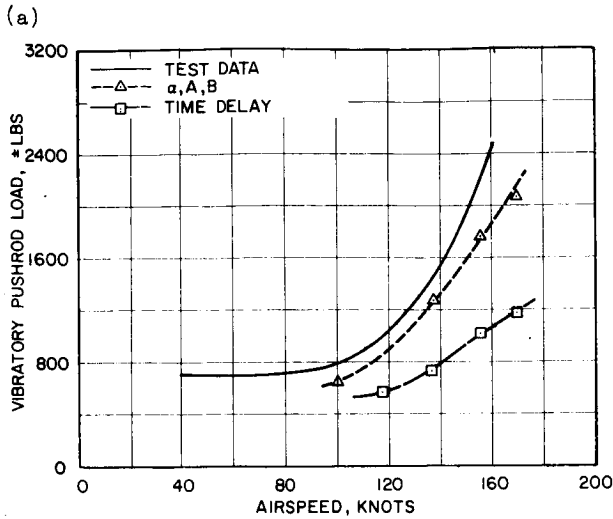


Figure 11. Correlation of CH-53A Vibratory Pushrod Loads.

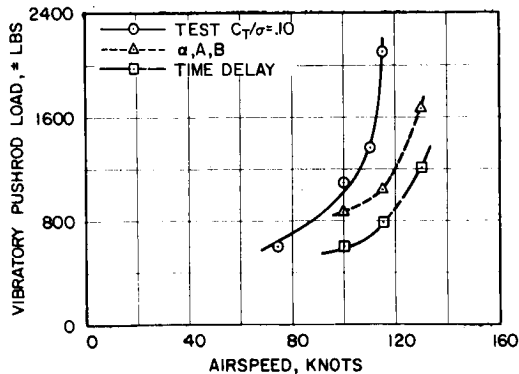


Figure 12. Correlation of CH-54B Vibratory Pushrod Loads.

that more negative pitch damping is present in the α, A, B results. Rather pitching moments along the blade are more in phase with each other, leading to larger modal excitation. In the α, A, B formulation, pitching moment coefficients are tabulated as functions of $\alpha, \dot{\alpha}$ and δ values all along the blade. This formulation leads to similarly phased pitching moments. In the Time Delay Model, moments are calculated based on the angles of attack exceeding the steady state stall angle for a certain interval of time and are not solely dependent on the instantaneous angle of attack characteristics. For small differences in calculated angles of attack, computed pitching moments for adjacent blade sections can be different in phase. Because the two-dimensional wind tunnel airfoil was modeled as a single panel for the calculation of aerodynamic forces, the effects of simultaneous spanwise stalling were not a factor in the correlation with that data.

Comparison of Methods

Because the α, A, B Method has demonstrated better correlation with flight test data, it continues to be the method in use for blade design analysis. However, development of both methods continues. The α, A, B Method provides a relatively direct and simple procedure for calculating unsteady aerodynamic loads. Correlation has been good with test data but its disadvantage centers largely on the apparent need for extensive tests to provide the body of tabulated data required for each airfoil. Some success has been obtained by scaling the NACA 0012 unsteady aerodynamic tables based on steady state differences between airfoils. Work is also being done on developing analytical expressions to replace the tabulated data. These may lead to the ability to synthesize the data required for a given airfoil, which would make the method more desirable for general applications.

The Time Delay Method has the great advantage of requiring only steady state airfoil data for its application. The correlation with forced oscillations of two-dimensional airfoils demonstrated its applicability over a wide range of conditions. Correlation with the tests described in this paper showed no clear advantage of the Time Delay Method over the α, A, B Method, and correlation with flight test data was definitely poorer with the Time Delay Method. Further work must be done to investigate the reasons for the poor flight test correlation. The problem may result from the assumption in the analysis that, on a blade, each radial section acts independently of its neighboring sections. This causes a more random stalling along the span with time, which smoothes out the changes in blade loading. The propagation of stall along the span for the three-dimensional case of a helicopter blade must be added to the Time Delay Method. The α, A, B Method does provide spanwise correlation in loading by use of torsional mode acceleration to calculate the B parameter. This acceleration is in phase for each point along the blade span. Incorporation of a suitable radial propagation model in the Time Delay Method may make this a more versatile, more easily applicable, and

more accurate model of unsteady aerodynamics. Until this can be shown the α , A, B Method continues in use in blade design.

Conclusions

1. The α , A, B and Time Delay unsteady aerodynamic models predict with good accuracy the lift and pitching moment hysteresis loops and the aerodynamic pitch damping of rigidly driven oscillating airfoils.
2. Two-dimensional stall flutter tests indicate that reducing blade torsional stiffness, reducing blade torsional inertia and moving blade pitch axis forward decrease stall flutter induced moments. Inception of stall flutter was delayed with the SC 1095 airfoil relative to the NACA 0012 airfoil; however, once initiated, stall flutter loads for the two airfoils were generally comparable.
3. Stall flutter response of the two-dimensional model airfoils and the effects of airfoil structural design parameters on blade torsional moments can be calculated using both unsteady models. The Time Delay method gives a high prediction of response amplitude.
4. Good correlation of CH-53A and CH-54B blade stresses and control loads was obtained with a rotor aeroelastic analysis employing variable rotor inflow and unsteady aerodynamics. Best correlation was achieved using the α , A, B unsteady model. The Time Delay method generally underpredicted full scale rotor stall flutter response.
5. The α , A, B model is in use for blade design analysis. Refinements to the Time Delay Method may make it a more versatile and more easily applied unsteady aerodynamic model.

References

1. Gormont, R. E., A MATHEMATICAL MODEL OF UNSTEADY AERODYNAMICS AND RADIAL FLOW FOR APPLICATION TO HELICOPTER ROTORS, USAAMRDL TR 72-67. U. S. Army Air Mobility Research and Development Laboratory, Fort Eustis, Virginia, May 1973.
2. Ericsson, L. E. and Reding, J. P., UNSTEADY AIRFOIL STALL REVIEW AND EXTENSION, AIAA Journal of Aircraft, Vol. 8, No. 8, August 1971.
3. McCroskey, W. J., RECENT DEVELOPMENTS IN ROTOR BLADE STALL, AGARD Conference Pre-Print No. 111 on Aerodynamics of Rotary Wings, September 1972.

4. Carta, F. O., Commerford, G. L., Carlson, R. G., and Blackwell, R. H., INVESTIGATION OF AIRFOIL DYNAMIC STALL AND ITS INFLUENCE ON HELICOPTER CONTROL LOADS, United Aircraft Research Laboratories; USAAMRDL TR 72-51, U. S. Army Air Mobility Research and Development Laboratory, Fort Eustis, Virginia, September 1972.
5. Gray, L. and Liiva, J., WIND TUNNEL TESTS OF THIN AIRFOILS OSCILLATING NEAR STALL, The Boeing Company, Vertol Division; USAAMRDL TR 68-89A and 68-89B, U. S. Army Aviation Materiel Laboratories, Fort Eustis, Virginia, January 1969.
6. Ham, N. D. and Garelick, M. S., DYNAMIC STALL CONSIDERATIONS IN HELICOPTER ROTORS, Journal of the American Helicopter Society, Vol. 13, No. 2, April 1968.
7. Tarzanin, F. J., PREDICTION OF CONTROL LOADS DUE TO BLADE STALL, American Helicopter Society, 27th Annual National Forum, May 1971.
8. Arcidiacono, P. J., Carta, F. O., Caselini, L. M., and Elman, H. L., INVESTIGATION OF HELICOPTER CONTROL LOADS INDUCED BY STALL FLUTTER, United Aircraft Corporation, Sikorsky Aircraft Division; USAAVLABS TR 70-2, U. S. Army Aviation Materiel Laboratories, Fort Eustis Virginia, March 1970.
9. Carta, F. O., and Niebanck, C. F., PREDICTION OF ROTOR INSTABILITY AT HIGH FORWARD SPEEDS, Volume III, STALL FLUTTER, USAAVLABS TR 68-18C, U. S. Army Aviation Materiel Laboratories, Fort Eustis, Virginia, February 1969.
10. Arcidiacono, P. J., PREDICTION OF ROTOR INSTABILITY AT HIGH FORWARD SPEEDS, Vol. I, Steady Flight Differential Equations of Motion for a Flexible Helicopter Blade with Chordwise Mass Unbalance, United Aircraft Corporation, Sikorsky Aircraft Division; USAAVLABS TR 68-18A, U. S. Army Aviation Materiel Laboratories, Fort Eustis, Virginia, February 1969.